

IMPRESSION - Prediction of NMR Parameters for 3-dimensional chemical structures using Machine Learning with near quantum chemical accuracy[†]

Will Gerrard, Lars Andersen Bratholm, Martin Packer, Adrian J. Mulholland, David R. Glowacki*, Craig P. Butts*

The IMPRESSION (Intelligent Machine PRediction of Shift and Scalar Information Of Nuclei) machine learning system provides an efficient and accurate route to the prediction of NMR parameters from 3-dimensional chemical structures. Here we demonstrate that machine learning predictions, trained on quantum chemical computed values for NMR parameters, are essentially as accurate but computationally much more efficient (tens of milliseconds per molecule) than quantum chemical calculations (hours/days per molecule). Training the machine learning systems on quantum chemical, rather than experimental, data circumvents the need for existence of large, structurally diverse, error-free experimental databases and makes IMPRESSION applicable to solving 3-dimensional problems such as molecular conformation and isomerism.

1 Introduction

NMR spectroscopy remains the pre-eminent analytical technique for elucidating molecular structure in solution, with the prediction and thus interpretation of ^1H and ^{13}C chemical shifts and scalar coupling constants playing a key role. The prediction of these parameters, especially in studies of 3-dimensional molecular structure, are increasingly moving towards quantitative comparison between computed values for proposed chemical structures and experiment. In such comparisons, the use of fast and accurate NMR prediction methods is crucial.

Fast empirical predictions of chemical shifts for 2-dimensional chemical structures have been used for decades, with the additivity rules exemplified by Pretsch¹ and HOSE-code² variants forming the basis of many analyses. However their accuracy is limited by being based on 2-dimensional structures and cannot readily deal with 3-dimensional conformational or stereochemical analysis. Some modifications to treating 3-dimensional structures have been made by e.g. flat-but-stereochemically-aware HOSE codes³ or single conformer models of experimental systems⁴⁻⁶ but the improvements in 3D accuracy are limited as conformation, and flexibility must necessarily be accounted for completely to achieve maximum accuracy. Multiple-bond ^1H - ^1H coupling constants are more directly linked to 3-dimensional structure, however, generically applicable Karplus-style empirical relationships, such as the widely used equation reported by Haasnoot *et al*⁷, suffer from lower accuracy when confronted with complex chemical functionality and equations designed for specific sub-structures, e.g. carbohydrates⁸, are not applicable to the whole of chemical

space. Finally, some NMR parameters, for example 1-bond ^1H - ^{13}C scalar coupling constants, $^1J_{\text{CH}}$, which are sensitive to both chemical connectivity *and* 3-dimensional structure are rarely used in isotropic studies precisely because there are no general empirical predictive methods for $^1J_{\text{CH}}$.

For all of these reasons, the accurate prediction of NMR parameters in modern 3-dimensional structure determinations relies increasingly on the use of quantum chemical calculations, typically based on Density Functional Theory (DFT)⁹⁻¹². Optimal DFT methods can be very accurate indeed, e.g. $^1J_{\text{CH}}$ predicted to within 1.5-4Hz (on values that range from roughly 100-300Hz)¹³⁻¹⁵ and $<0.2/ <2\text{ppm}$ ^{16 17} (on ranges of 10 and 200ppm) for $\delta^1\text{H}$ and $\delta^{13}\text{C}$ chemical shifts respectively. The substantial downside of DFT is the significant computation time required when using methods that can provide sufficient accuracy in NMR predictions. Accurate DFT-based NMR predictions typically take hours to days of CPU time for even relatively small molecules of 500 molecular mass. In cases where multiple conformers or isomers must be considered this becomes days to months of computation for a single study.

Machine learning methods offer a solution to the time-demands of DFT calculation with each prediction conducted in seconds rather than hours or days. In NMR, machine learning predictions, trained on experimental data, of ^1H and ^{13}C chemical shifts based on 2-dimensional structures are well-established^{18 19 20 21}. These systems are trained on hundreds of thousands of validated experimental chemical shifts arising from tens of thousands of chemical structures. Such training datasets are less practical for scalar couplings because accurate and validated experimental databases do not exist on this scale (e.g. $^1J_{\text{CH}}$ values) and they can be critically dependent on 3-dimensional structure

University of Bristol, Bristol

[†] Electronic Supplementary Information (ESI) available: See DOI: XXX

(e.g. ${}^3J_{\text{HH/CH}}$ values). On the other hand, a machine could be trained using large datasets of DFT-computed values derived from 3-dimensional structures. Such large DFT-derived datasets can be generated systematically with minimal effort and are not limited to offering accuracy only for structures that are similar to previously experimentally determined molecules. With a large enough training database, such a machine would be expected to approach the accuracy of DFT calculation of NMR parameters for 3D structure analysis, but with several orders of magnitude reduction in time. This approach was recently reported for solid-state chemical shift predictions by Paruzzo *et al* (SHIFTML²²) where the computational demand of DFT calculations on extended lattices are comparably high to those of multi-conformer calculations on solution-state systems.

In this paper we describe the development of our first generation of solution-state NMR prediction machines - IMPRESSION (Intelligent Machine PREdiction of Shift and Scalar Information of Nuclei), trained on DFT-predicted values rather than relying on scarce or error-prone experimental data. We have chosen to demonstrate the versatility of machine learning of NMR parameters using both ${}^1\text{H}$ and ${}^{13}\text{C}$ chemical shifts and ${}^1J_{\text{CH}}$ couplings. We focus particularly on the latter as this is a parameter which is rarely used precisely because it is difficult to predict/interpret without DFT, and yet has been demonstrated to be valuable for elucidating both 2-dimensional connectivity and 3-dimensional structure^{5,23}. Providing a fast and accurate predictive tool will be especially valuable for this and could encourage wider acceptance of this parameter in structure determinations. We demonstrate that IMPRESSION can predict these NMR parameters for organic molecules, including 3-dimensional discrimination, with near-DFT accuracy but several orders of magnitude faster and can be applied to experimental data with essentially identical outcomes to DFT.

2 Results and Discussion

2.1 Dataset Production and Framework

In order to train and test IMPRESSION, we developed a dataset of NMR parameters, computed using DFT in the Gaussian software²⁴. While more demanding computational methods could be considered²⁵, their computational cost would be extortionate with minimal improvement in outcomes for the training and testing datasets described. Instead we found *MPW1PW91/6-311g(d,p)//wb97xd/6-311g(d,p)*²⁶⁻³⁰ to be computationally efficient and sufficiently accurate for comparison to experimental values, *vide infra*, across a range of NMR parameters so used this DFT method throughout this study. A training set of 882 structures (17,222 ${}^1J_{\text{CH}}$; 18,383 $\delta^1\text{H}$; 17,081 $\delta^{13}\text{C}$ values/environments) were selected by an adaptive sampling (active learning) procedure³¹⁻³³ from a superset of 75,382 chemical structures comprising only C, H, N, O and F atoms in the Cambridge Structural Database (accessed 7/9/2018). The adaptive sampling procedure trains an initial IMPRESSION machine from 100 chemical structures and then uses this machine to predict the parameters for all remaining structures in the superset to measure their variance in a 5-fold cross validation (*i.e.* how

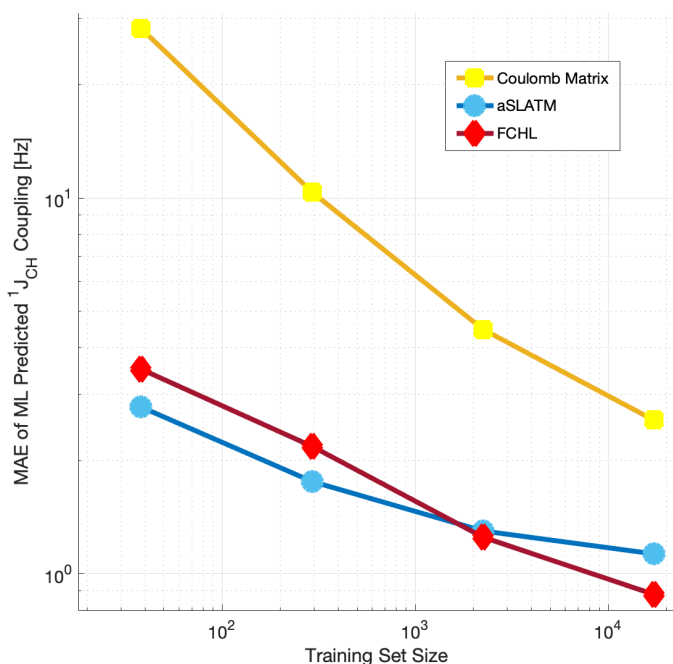


Fig. 1 Log-log plot of training set size vs accuracy of ${}^1J_{\text{CH}}$ coupling predictions on the test set for the Coulomb Matrix, aSLATM and FCHL kernel similarity measure.

much a given parameter changes when predicted from 5 separate machines each trained on a different 80% subset of the current training set). The 100 structures in the superset which show the highest variance are then added to the training dataset and the cycle is iterated (see Supplementary Information for further details). Adaptive sampling therefore adds the 100 structures at each training iteration which IMPRESSION is the most uncertain about. In doing so, each added structure provides the maximum information for training and substantially reduces the overall computational cost required to reach a given accuracy. The test set, against which the quality of the IMPRESSION predictions is independently tested, was comprised of a further 410 chemical structures (7832 ${}^1J_{\text{CH}}$; 8475 $\delta^1\text{H}$; 7523 $\delta^{13}\text{C}$ environments) harvested from the CSD-500 dataset recently reported by Paruzzo *et al*²².

IMPRESSION uses a Kernel Ridge Regression³⁴ (KRR) framework to learn the ${}^1J_{\text{CH}}$ scalar couplings and ${}^{13}\text{C}$ and ${}^1\text{H}$ chemical shifts of molecules. KRR was successfully used by Paruzzo *et al* to predict solid-state chemical shifts (SHIFTML²²). Neural networks have also been used to predict chemical shifts in small molecules from experimental data^{6,35,36}, however, we found no clear advantages in using feed forward neural networks in this work as the accuracy was comparable to KRR for the datasets used, with the kernel methods being much faster to train with the given training set size. In order to encode the similarity between chemical environments of each molecule we tested three approaches previously described - Coulomb matrices³⁷, aSLATM³⁸ and FCHL³⁹, all available from the QML python package⁴⁰. Both aSLATM and FCHL were found to outperform Coulomb matrices (Figure 1), which is due to Coulomb matrices neglecting three-body interactions. FCHL was substantially more computationally

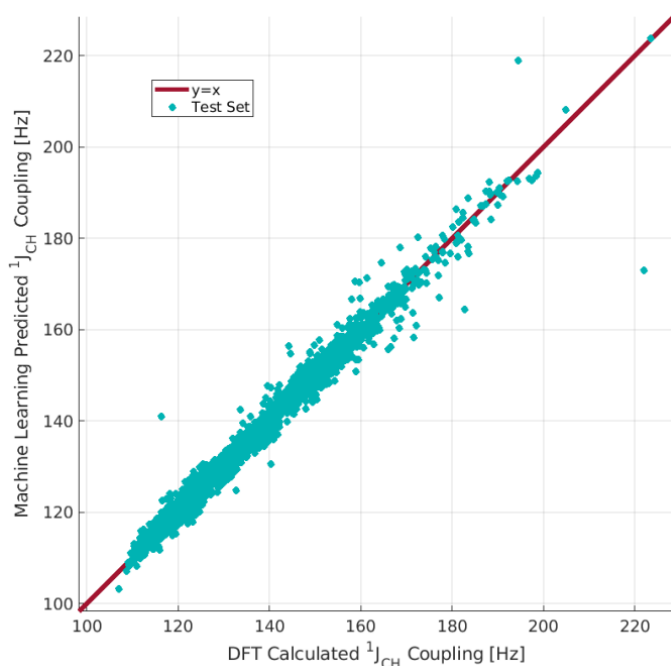


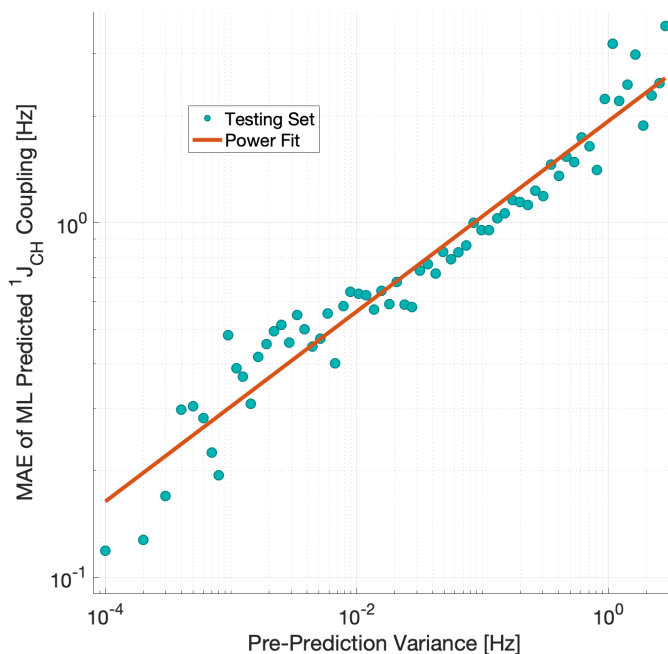
Fig. 2 DFT computed $^1J_{CH}$ coupling constants compared to IMPRESSION machine learning predictions without variance filtering.

efficient than aSLATM and thus was used in the final development of the full IMPRESSION machine. All of these kernel similarity measures compare *atomic* environments, so in the case of $^1J_{CH}$, we used the product of the separately calculated kernel similarities for the 1H and ^{13}C nuclei as this performed better than either atomic environment alone. The KRR procedure is further described in the Supplementary Information.

2.2 Performance versus DFT

During training, the machine performance improves steadily with increasing training set size, shown in Figure 1 for prediction of $^1J_{CH}$. This indicates that the accuracy can be further improved by adding additional training data, however the absolute gains at this point become marginal with a ten-fold increase in training set size approximately halving the average error between IMPRESSION and DFT. Using the full training set of 17,222 $^1J_{CH}$ environments, IMPRESSION achieved a mean absolute error (MAE) of 0.88Hz and a root mean squared error (RMSE) of 1.50Hz on the test set.

Notably however, a very small number of $^1J_{CH}$ predictions for the test set were much less reliable as clearly apparent in Figure 2, with 14 of the 7832 predicted $^1J_{CH}$ values (<0.2%) having deviations of >10Hz and the maximum error (MaxE) between IMPRESSION and DFT being 49.07Hz. These poorly predicted values are likely to arise from poor descriptions of rare $^1H/^{13}C$ chemical environments amongst the hundreds of molecular structures used to train IMPRESSION. We can *a priori* identify any poorly described environments using the same variance-based approach used to generate the training set. By assessing the variance in prediction of $^1J_{CH}$ for each environment across a 5-fold cross-validation, we are able estimate our confidence in



| Variance [Hz] | Envs | MAE [Hz] | RMSE [Hz] | MaxE [Hz] |
|----------------|------|----------|-----------|-----------|
| $10 > V > 100$ | 11 | 10.61 | 18.56 | 49.07 |
| $1 > V > 10$ | 157 | 2.78 | 3.94 | 18.31 |
| $0.1 > V > 1$ | 2143 | 1.25 | 1.73 | 11.33 |
| < 0.1 | 5521 | 0.66 | 0.95 | 13.37 |

Fig. 3 Top: correlation between pre-prediction variance and prediction error between DFT and IMPRESSION for $^1J_{CH}$ on the test set. The prediction errors were binned by variance and an average error (MAE) was produced for each bin. Bottom: error metrics for different variance ranges.

the predictions, as environments which are poorly described by the chemical structures in the training set will be likely have high variance in this cross-validation. There is indeed a clear correlation of variance against prediction error for the independent test set (Figure 3) suggesting that the cross-validation allows us to place a quantitative level of confidence on the predicted $^1J_{CH}$ values. The table and plot in Figure 3 illustrates the quality of fit for ranges of variance, and there is a substantial loss of accuracy for the small number of predictions with variance >10Hz.

Simply removing $^1J_{CH}$ values which show high variances in cross-validation can thus provide a "pre-prediction variance filter" which improve the quality, and thus the confidence, of IMPRESSION predictions. Removing the 11 couplings with pre-prediction variances of >10Hz improved the fit for the remaining test set values to MAE = 0.87Hz, RMSE = 1.33Hz and MaxE = 18.31Hz when compared to their original DFT values. Hence applying a variance filter based on the 5-fold cross-validation of each value compensates well for deficiencies in chemical space covered during the training of IMPRESSION, at the cost of not returning predictions for a very small number of environments. A similar training and test process (see Supplementary Information for details) was used for δ^{1H} and δ^{13C} values, resulting in satisfactory fits to DFT (MAE = 0.22ppm/2.16ppm; RMSE = 0.3/3.24ppm; MaxE = 2.16/32.3ppm) on the test set after variance filtering.

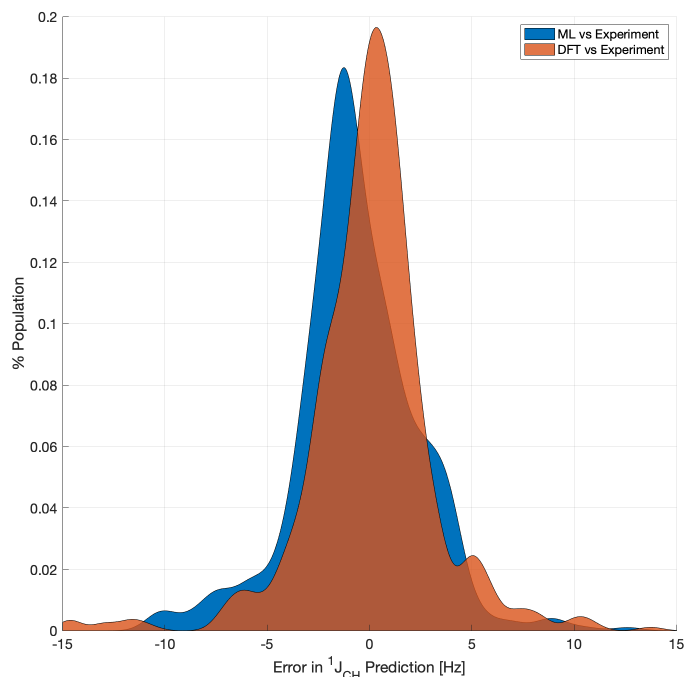


Fig. 4 Distribution of errors for machine learning $^1J_{\text{CH}}$ predictions (variance filter $>5\text{Hz}$ applied) and DFT calculations for the experimental validation dataset.

The performance of IMPRESSION with respect to DFT compares very well with that of DFT with respect to experiment. Buevich *et al* recently highlighted that current best-in-class DFT methods predict $^1J_{\text{CH}}$ experimental values with accuracies of 2-4Hz, when presenting an optimised workflow for calculating $^1J_{\text{CH}}$ values which achieved an RMSE of 1.61Hz. Similarly, $\delta^1\text{H}$ and $\delta^{13}\text{C}$ chemical shift predictions with optimal DFT methods provide accuracies down to $<0.2/ <2\text{ppm}$ ^{16 17} with respect to experiment. Consequently, the results for IMPRESSION with the test set suggest that it can reproduce DFT values with comparable accuracies to that with which the current best DFT methods can reproduce experimental values.

2.3 Performance versus Experiment

Naturally, the key test of IMPRESSION is its ability to directly reproduce experimental values of relevant compounds. To test this for $^1J_{\text{CH}}$, a validation set of 608 experimental $^1J_{\text{CH}}$ values were taken from structures collated by Venkata *et al*²³ which contain C, H, N, O and F elements only. Firstly, we checked the ability of our $\omega\text{b97xd}/6\text{-311g(d,p)}$ DFT method itself to reproduce these experimental results. Calculating the 608 couplings with $\omega\text{b97xd}/6\text{-311g(d,p)}$ took 156 CPU hours and initially gave a relatively poor fit to experiment (MAE = 10.92Hz) but with a systematic offset from the experimental data by an average of -10.91Hz. A simple additive correction of +10.91Hz to the DFT-predicted values provided a good fit between DFT and experiment (MAE = 2.15Hz; RMSE = 3.33Hz; MaxE = 20.05Hz) and this was used for all subsequent comparisons to experiment based on this DFT method. As IMPRESSION is trained on DFT data computed with this same $\omega\text{b97xd}/6\text{-311g(d,p)}$ method, these statistics represent

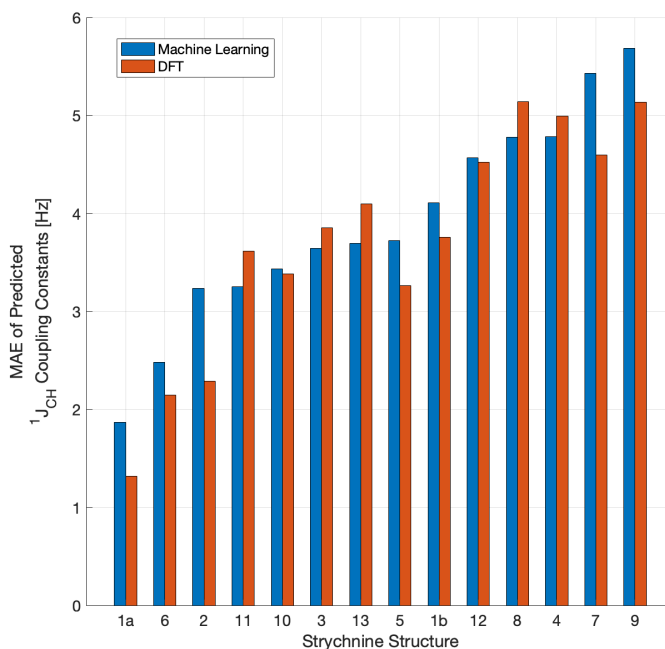


Fig. 5 MAE between experiment and predictions of $^1J_{\text{CH}}$ for 13 diastereomers of strychnine (including two structures for the natural product 1: the lowest energy conformer 1a ($>97\%$ populated) and next lowest energy conformer 1b ($<3\%$ populated)).

a practical limit for the accuracy that we might expect from IMPRESSION on this experimental data. There are many sources of error in DFT NMR calculations⁴¹⁻⁴³ including the effects of solvent models and conformational averaging of NMR parameters (neither of which were corrected for directly beyond the simple linear corrections). Work is ongoing to reduce these errors in the production of our datasets.

IMPRESSON took only 60 CPU seconds to predict the full set of 608 $^1J_{\text{CH}}$ values but with some substantial outliers (MAE = 3.69Hz; RMSE = 7.18Hz; MaxE = 54.36Hz). Applying a $>10\text{Hz}$ variance filter removed 44 values and substantially improved the fit between IMPRESSION and the experimental values (MAE = 2.47Hz ; RMSE = 3.22Hz; MaxE = 12.63Hz). A tighter $>5\text{Hz}$ filter, removed 12 additional values and was found to provide essentially identical accuracy to the DFT method for the remaining 552 values (MAE = 2.31Hz; RMSE = 2.93Hz; MaxE = 12.63Hz). An overlay of the error distributions for DFT and the $>5\text{Hz}$ variance-filtered IMPRESSION vs the experimental values (Figure 4) demonstrates the comparability between machine learning and DFT. This represents quite excellent performance of the machine for reproducing experimental data in just a few seconds, but with comparable quality to the 1.5-4Hz MAEs described by Buevich *et al* as typical for DFT methods, with $<10\%$ of the values being tagged as unreliable by the variance filter.

2.4 3-Dimensional Structure Discrimination

A demanding test of IMPRESSION is in its ability to predict and discriminate experimental NMR data for stereoisomeric compounds i.e. those that differ only in their 3-dimensional structure, but not connectivity. This is especially challenging because

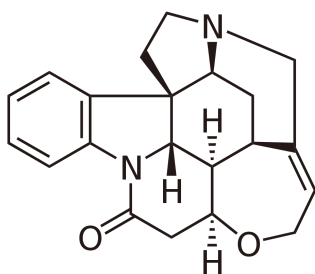


Fig. 6 Structure of the natural product strychnine **1**

IMPRESSION has not been explicitly trained to deal with multiple conformers/isomers of a compound. Instead 3-dimensional variation is only implicit within the varied chemical structural space of the adaptively sampled training set. Buevich *et al* recently demonstrated⁵ that DFT prediction of $^1J_{CH}$ values can successfully discriminate the naturally occurring structure **1** of the polycyclic alkaloid strychnine (Figure 6) from 12 other diastereomers (see Supplementary Information for the structures) based on comparison with the experimental $^1J_{CH}$ values of the natural product. Pleasingly, the same test conducted with IMPRESSION-predicted $^1J_{CH}$ values (blue bars in Figure 5) also correctly identifies the natural product diastereomer **1a** as having the best fit (MAE = 1.87Hz; RMSE = 2.50Hz; MaxE = 6.19Hz). The fit for the correct structure is 30% better than the next best fitting diastereomer **6** (MAE = 2.48Hz; RMSE = 3.38Hz; MaxE = 8.42Hz) and this is very similar to the discrimination offered by ω b97xd/6-311g(d,p) (red bars in Figure 5). Indeed IMPRESSION could also distinguish between the 3-dimensional structures of **1a**, the lowest energy conformer of the natural product (97% population in solution), and **1b** which is the second lowest energy conformer (3% population in solution)⁴⁴. So while the absolute accuracy of IMPRESSION for predicting $^1J_{CH}$ values for strychnine (MAE = 1.87Hz) is slightly lower than that obtained from the DFT method (MAE = 1.31Hz), its discriminating power between structural isomers is nearly the same.

It is interesting to note that combining $^1J_{CH}$ with IMPRESSION predictions of 1H and ^{13}C chemical shifts also provides discrimination of the naturally occurring structure, but that IMPRESSION and DFT now both see structure **2** as the next best fit. This arises from the DFT 1H chemical shift prediction, where it identifies the lowest the best fit to be for incorrect diastereomer **2** - and IMPRESSION demonstrates exactly the same 'mistake'. This suggests that IMPRESSION is indeed a very rapid and robust method for reproducing the quality of results of a quantum chemistry method - whether the given quantum chemistry method can correctly reproduce experiment or not *i.e.* if improved quantum chemical calculations are provided to train the machine, then the performance of the machine will improve in line with this.

3 Conclusions

In summary, this first generation IMPRESSION machine, trained on DFT-computed NMR parameters derived from a set of 3-dimensional structures is capable of reproducing DFT-predicted NMR parameters with high accuracy, but in a fraction of the

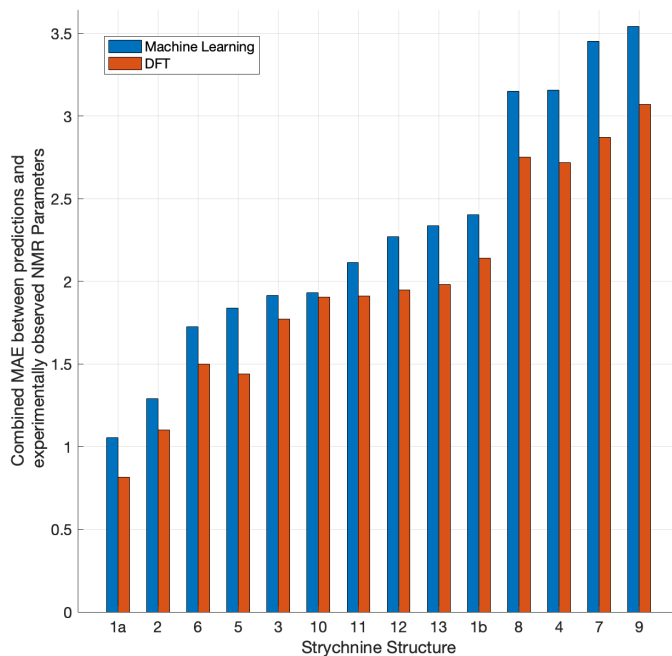


Fig. 7 Combined MAE (geometric mean) between experiment and predictions of $^1J_{CH}$, δ^1H , and $\delta^{13}C$ for 13 diastereomers of strychnine (including two structures for the natural product **1**: the lowest energy conformer **1a** (>97% populated) and next lowest energy conformer **1b** (<3% populated).

time. Accurate and generalised prediction of NMR parameters for 3-dimensional applications has not been addressed by previous machine learning systems but the confidence provided by the variance-filtered IMPRESSION results makes this tool essentially as robust for 3D applications to experimental systems as DFT. At this stage, the two primary sources of error in IMPRESSION predictions of experimental data are the accuracy of the underlying DFT method from which it is trained and the range of chemical space covered by the current IMPRESSION training set. We are working to improve both of these factors, as well as extending the predictions to multiple-bond scalar couplings for future generations of IMPRESSION, along with developing a more rigorous statistical treatment of the predicted values taking into account the pre-prediction variance.

Conflicts of interest

There are no conflicts to declare.

Acknowledgements

This work was carried out using the computational facilities of the Advanced Computing Research Centre, University of Bristol - <http://www.bristol.ac.uk/acrc/>. We thank Dr Peter Howe (Syngenta, UK) for useful discussions regarding the experimental $^1J_{CH}$ dataset used. WG thanks the EPSRC National Productivity Investment Fund (NPIF) for Doctoral Studentship funding. LAB thanks the Alan Turing Institute under the EPSRC grant EP/N510129/1. DRG acknowledges funding from the Royal Society as a University Research Fellow, and also from EPSRC grant EP/M022129/1. AJM thanks EPSRC for funding (EP/M022609/1,

CCP-BioSim). LAB and DRG acknowledge support of this work through EPSRC grant EP/P021123/1. We further acknowledge the use of the following software: BayesianOptimization⁴⁵, OpenBabel⁴⁶, Pybel⁴⁷, NumPy⁴⁸, OpenMP⁴⁹, F2PY⁵⁰.

Notes and references

- 1 E. Pretsch, T. Clerc, J. Seibl and W. Simon, *Tables of spectral data for structure determination of organic compounds*, Springer Science & Business Media, 2013.
- 2 W. Bremser, *Anal. Chim. Acta*, 1978, **103**, 355–365.
- 3 S. Kuhn and S. R. Johnson, *ACS Omega*, 2019, **4**, 7323–7329.
- 4 J. Aires-de Sousa, M. C. Hemmer and J. Gasteiger, *Anal. Chem.*, 2002, **74**, 80–90.
- 5 A. V. Buevich, J. Saurí, T. Parella, N. De Tommasi, G. Bifulco, R. T. Williamson and G. E. Martin, *Chem. Commun.*, 2019, **55**, 5781–5784.
- 6 J. Meiler, W. Maier, M. Will and R. Meusinger, *J. Mag. Reson.*, 2002, **157**, 242–252.
- 7 C. Haasnoot, F. A. de Leeuw and C. Altona, *Tetrahedron*, 1980, **36**, 2783–2792.
- 8 B. Coxon, *Adv. Carbohydr. Chem. Biochem.*, 2009, **62**, 17–82.
- 9 A. Navarro-Vázquez, *Magn. Reson. Chem.*, 2017, **55**, 29–32.
- 10 M. W. Lodewyk, M. R. Siebert and D. J. Tantillo, *Chem. Rev.*, 2011, **112**, 1839–1862.
- 11 C. Steinmann, L. A. Bratholm, J. M. H. Olsen and J. Kongsted, *J. Chem. Theory Comput.*, 2017, **13**, 525–536.
- 12 A. S. Larsen, L. A. Bratholm, A. S. Christensen, M. Channir and J. H. Jensen, *PeerJ*, 2015, **3**, e1344.
- 13 T. Helgaker, M. Jaszuński and M. Pecul, *Prog. Nucl. Magn. Reson. Spectrosc.*, 2008, **4**, 249–268.
- 14 S. N. Maximoff, J. E. Peralta, V. Barone and G. E. Scuseria, *J. Chem. Theory Comput.*, 2005, **1**, 541–545.
- 15 J. F. San, J. de la Vega García, R. Suardiáz, M. Fernández-Oliva, C. Pérez, R. Crespo-Otero and R. Contreras, *Magn. Reson. Chem.*, 2013, **51**, 775–787.
- 16 N. Grimblat, M. M. Zanardi and A. M. Sarotti, *J. Org. Chem.*, 2015, **80**, 12526–12534.
- 17 V. A. Semenov and L. B. Krivdin, *Magn. Reson. Chem.*, 2019.
- 18 *NMR Prediction Software from ACD/Labs*, https://www.acdlabs.com/products/adh/nmr/nmr_pred/.
- 19 *NMR Prediction Software from Mestrelab*, <https://mestrelab.com/software/mnova/nmr-predict/>.
- 20 A. M. Castillo, A. Bernal, R. Dieden, L. Patiny and J. Wist, *J. Cheminf.*, 2016, **8**, 26.
- 21 A. J. Brandolini, *NMRPredict Modgraph Consultants, Ltd, 1348 Graham Place, Escondido, CA 92129*. <http://www.modgraph-usa.com>, 2006.
- 22 F. M. Paruzzo, A. Hofstetter, F. Musil, S. De, M. Ceriotti and L. Emsley, *Nat. Commun.*, 2018, **9**, 4501.
- 23 C. Venkata, M. J. Forster, P. W. Howe and C. Steinbeck, *PLoS one*, 2014, **9**, e111576.
- 24 M. Frisch, G. Trucks, H. Schlegel, G. Scuseria, M. Robb, J. Cheeseman, G. Scalmani, V. Barone, B. Mennucci, G. Pettersson *et al.*, Wallingford, CT, 2009.
- 25 A. M. Teale, O. B. Lutnæs, T. Helgaker, D. J. Tozer and J. Gauss, *J. Chem. Phys.*, 2013, **138**, 024111.
- 26 C. Adamo and V. Barone, *J. Chem. Phys.*, 1998, **108**, 664–675.
- 27 A. McLean and G. Chandler, *J. Chem. Phys.*, 1980, **72**, 5639–5648.
- 28 R. Krishnan, J. S. Binkley, R. Seeger and J. A. Pople, *J. Chem. Phys.*, 1980, **72**, 650–654.
- 29 J.-D. Chai and M. Head-Gordon, *J. Chem. Phys.*, 2008, **128**, 084106.
- 30 W. Deng, J. R. Cheeseman and M. J. Frisch, *J. Chem. Theory Comput.*, 2006, **2**, 1028–1037.
- 31 H. S. Seung, M. Opper and H. Sompolinsky, Proc. 5th Ann. Work. Comp. Learn. Theory, New York, NY, USA, 1992, pp. 287–294.
- 32 M. Gastegger, J. Behler and P. Marquetand, *Chem. Sci.*, 2017, **8**, 6924–6935.
- 33 J. S. Smith, B. Nebgen, N. Lubbers, O. Isayev and A. E. Roitberg, *J. Chem. Phys.*, 2018, **148**, 241733.
- 34 C. Saunders, A. Gammerman and V. Vovk, 1998.
- 35 Y. Binev and J. Aires-de Sousa, *J. Chem. Inf. Comput. Sci.*, 2004, **44**, 940–945.
- 36 Y. Binev, M. M. Marques and J. Aires-de Sousa, *J. Chem. Inf. Model.*, 2007, **47**, 2089–2097.
- 37 M. Rupp, R. Ramakrishnan and O. A. Von Lilienfeld, *J. Phys. Chem. Lett.*, 2015, **6**, 3309–3313.
- 38 B. Huang and O. A. von Lilienfeld, *arXiv preprint arXiv:1707.04146*, 2017.
- 39 F. A. Faber, A. S. Christensen, B. Huang and O. A. von Lilienfeld, *J. Chem. Phys.*, 2018, **148**, 241717.
- 40 A. S. Christensen, L. A. Bratholm, S. Amabilino, J. C. Kromann, F. A. Faber, B. Huang, A. Tkatchenko, K. R. MÅijller and O. A. von Lilienfeld, *QML: A Python Toolkit for Quantum Machine Learning*, 2019, <https://github.com/qmlcode/qml>.
- 41 M. A. Iron, *J. Chem. Theory Comp.*, 2017, **13**, 5798–5819.
- 42 A. Bagno, F. Rastrelli and G. Saielli, *Chemistry—A European Journal*, 2006, **12**, 5514–5525.
- 43 R. Laskowski, P. Blaha and F. Tran, *Physical Review B*, 2013, **87**, 195130.
- 44 C. P. Butts, C. R. Jones and J. N. Harvey, *Chem. Commun.*, 2011, **47**, 1193–1195.
- 45 F. Nogueira, *A Python implementation of global optimization with gaussian processes*, 2019, <https://github.com/fmfn/BayesianOptimization>.
- 46 N. M. O’Boyle, M. Banck, C. A. James, C. Morley, T. Vandermeersch and G. R. Hutchison, *J. Cheminf.*, 2011, **3**, 33.
- 47 N. M. O’Boyle, C. Morley and G. R. Hutchison, *Chem. Cent. J.*, 2008, **2**, 5.
- 48 T. E. Oliphant, *A guide to NumPy*, Trelgol Publishing USA, 2006, vol. 1.
- 49 L. Dagum and R. Menon, *Comput. Sci. Eng.*, 1998, 46–55.
- 50 P. Peterson, *Int. J. Comput. Sci. Eng.*, 2009, **4**, 296–305.